

# Mössbauer evidence of $^{57}\text{Fe}_3\text{O}_4$ based ferrofluid biodegradation in the brain

D. Polikarpov · V. Cherepanov · M. Chuev ·  
R. Gabbasov · I. Mischenko · M. Nikitin · Y. Vereshagin ·  
A. Yurenia · V. Panchenko

© Springer Science+Business Media Dordrecht 2014

**Abstract** The ferrofluid, based on  $^{57}\text{Fe}$  isotope enriched  $\text{Fe}_3\text{O}_4$  nanoparticles, was synthesized, investigated by Mössbauer spectroscopy method and injected transcranially in the ventricle of the rat brain. The comparison of the Mössbauer spectra of the initial ferrofluid and the rat brain measured in two hours and one week after the transcranial injection allows us to state that the synthesized magnetic  $^{57}\text{Fe}_3\text{O}_4$  nanoparticles undergo intensive biodegradation in live brain and, therefore, they can be regarded as a promising target for a new method of radionuclide-free Mössbauer brachytherapy.

**Keywords** Mössbauer spectroscopy · Magnetic nanoparticles · Brain

## 1 Introduction

Nowadays, radiotherapy is the most effective means of tumor control. Radiotherapy makes use either of external sources of penetrating radiation or of administered radioisotopes. Both methods have essential deficiencies. In the former case, it irreversibly affects not only

---

Proceedings of the 32nd International Conference on the Applications of the Mössbauer Effect (ICAME 2013) held in Opatija, Croatia, 1–6 September 2013

D. Polikarpov (✉) · V. Cherepanov · R. Gabbasov · Y. Vereshagin · A. Yurenia · V. Panchenko  
National Research Centre, Kurchatov Institute, Moscow, Russia  
e-mail: polikarpov.imp@gmail.com

A. Yurenia · V. Panchenko  
Lomonosov Moscow State University, Moscow, Russia

M. Chuev · I. Mischenko  
Institute of Physics and Technology, Russian Academy of Sciences, Moscow, Russia

M. Nikitin  
Shemyakin-Ovchinnikov Institute of Bioorganic Chemistry, Russian Academy of Sciences,  
Moscow, Russia

pathological, but also healthy tissues which the radiation passes through. The second alternative related to the target delivery of radioactive preparation immediately to the affected organ requires administering of larger doses of highly radioactive radionuclides into the body and is accompanied by irreversible toxic action of non-removable decay products of these radionuclides on the patient's health. Therefore, it is an urgent imperative to develop new methods of radiotherapy free of deficiencies of both current approaches: it must ensure local exposure of the pathological area without affecting surrounding tissues and at the same time it cannot necessitate administering radionuclides into a patient's organism. One of the known solutions consists in the use of resonance interaction of external X-rays with targets address-deliverable to the affected organ. Herewith, the task is set to minimize the biological action of primary X-rays and to maximize the biological action of secondary radiations generated by the target under the action of external radiation. The target can be introduced into the intended organ directly with a hollow needle [1] or using the methods of target delivery of medicines. In the latter case, the irradiated target can be made of magnetic nanoparticles, and the fact of their delivery to the intended organ can be visualized with magnetic-resonance tomography (MRT) [2].

It has been suggested that secondary radiations accompanying resonance absorption of Mössbauer radiation in  $^{57}\text{Fe}$  nuclei may be capable of producing a highly effective local effect on biological tissues [3]. The latter circumstance results from the fact that the excited nucleus decay after the quantum Mössbauer absorption is accompanied by a cascade of Auger- or low-energy (of the order of 1 keV) conversion electrons which have much higher biological efficiency than primary quanta. Therefore, a therapeutic method based on the use of secondary radiations excited in a biodegradable nanodimensional ferriferrous target by primary radiation from an exterior Mössbauer source could potentially be an instrument for targeted interstitial radiation of neoplasms. However, it should also be mentioned here, that the application of radionuclide-free Mössbauer brachytherapy is still strongly debated [4].

Of late, a vigorous growth of investigations of iron-containing magnetic nanoparticles for biomedical applications has been observable owing to their prompt biodegradability in a live organism with the formation of endogenous iron-containing proteins, such as ferritin and hemoglobin. Since no side effects were revealed in the course of clinical trials, magnetic ferrofluids based on  $\text{Fe}_3\text{O}_4$  magnetite nanoparticles are being widely spread by pharmaceutical companies as a standard medical preparation for MRT pattern contrast enhancement. Besides, an active work is under way aimed at the development of medical technologies based on nanomagnetic materials, such as the targeted magnetic delivery of pharmaceutical products, controllable magnetic blood-vessel thrombosing, tumor hyperthermia through magnetic particle heating in a variable magnetic field. Therefore, the application of conglomerates of magnetite magnetic nanoparticles as biodegradable targets address-deliverable to the intended organ is promising for radionuclide-free Mössbauer brachytherapy. Since the content of the Mössbauer isotope in natural iron is 2 %, such nanoparticles must be synthesized from iron enriched in the  $^{57}\text{Fe}$  isotope. The ferrofluids produced on their basis must be biocompatible, i.e., suitable for injections, and they must be biodegradable in a live organism. This paper reports on the results of activities aimed at the synthesis of  $^{57}\text{Fe}_3\text{O}_4$  nanoparticles with increased  $^{57}\text{Fe}$  content meeting these requirements.

## 2 Synthesis of the ferrofluid based on the magnetic $\text{Fe}_3\text{O}_4$ nanoparticles with increased content of the $^{57}\text{Fe}$ isotope

As was earlier noted, the biodegradability of the ferrofluids based on  $\text{Fe}_3\text{O}_4$  nanoparticles and their complete excretion from a live organism depend crucially on a method of their synthesis. In ref. [5], a magnetic iron-containing ferrofluid was administered into a cerebral cavity of a rat by a direct transcranial injection. Three months later the brain was extracted and analyzed with the histological and Mössbauer spectroscopy methods. It was found that  $\text{Fe}_3\text{O}_4$  nanoparticles which comprised 92 % of all the iron content of the ferrofluid had completely biodegraded or had been excreted from the brain, while the iron chemical compound attending the process of ferrofluid synthesis remained intact in the brain. For this reason, the method of Mössbauer spectroscopy was employed in this investigation for the close control of the chemical composition homogeneity during the synthesis of the isotopically-enriched  $^{57}\text{Fe}_3\text{O}_4$ -based ferrofluid at every stage of the process.

$\text{Fe}_3\text{O}_4$  magnetic nanoparticles were synthesized with the sol-gel process by co-precipitation of water solution of hydrate of iron chloride  $\text{FeCl}_2 \cdot 4\text{H}_2\text{O}$  and solution of  $\text{FeCl}_3$  in 0.1 M HCl ( $\text{Fe}^{2+}:\text{Fe}^{3+} = 1:2$ ) in 30 % solution of ammonium hydroxide,  $\text{NH}_4\text{OH}$ . After incubation at 90 °C, the particles underwent magnetic separation and flushing in 2 M  $\text{HNO}_3$  followed by their introduction into distilled  $\text{H}_2\text{O}$  to form a suspension. The as-produced suspension was supplemented with 70 kDa dextran from *Leuconostoc* spp. (Sigma, USA). After re-incubation at 80 °C, the particles were triply flushed in  $\text{dH}_2\text{O}$  by centrifuging. Then the particles were sorted for the selection of batches of particles with similar dimensions.

The application of the traditional sol-gel procedure for preparation of the isotopically-enriched  $^{57}\text{Fe}_3\text{O}_4$  nanoparticles requires availability of initial hydrates of both trivalent and divalent iron chloride enriched in the  $^{57}\text{Fe}$  stable isotope. The initial raw material the authors had at their disposal was  $\alpha$ - $^{57}\text{Fe}_2\text{O}_3$  compound with 96 % enrichment in the  $^{57}\text{Fe}$  stable isotope containing iron in the trivalent state. Trivalent  $^{57}\text{FeCl}_3$  was synthesized by direct solving  $\alpha$ - $^{57}\text{Fe}_2\text{O}_3$  in HCl. Synthesis of divalent  $\text{FeCl}_2$  from  $\alpha$ - $^{57}\text{Fe}_2\text{O}_3$  is possible, but should be carried out in two stages. First, one has to get the iron metal by reduction of  $\alpha$ - $^{57}\text{Fe}_2\text{O}_3$  in hydrogen at  $T = 800$  °C. Then it is necessary to dissolve metallic iron in the HCl in an oxygen free atmosphere. In view of engineering problems of the first stage, it was decided to be restricted in the framework of this investigation to the synthesis of trivalent  $^{57}\text{FeCl}_3$  only with its subsequent co-precipitation with  $\text{FeCl}_2 \cdot 4\text{H}_2\text{O}$  of the natural isotope composition in the 2:1 ratio. As a result the as-produced  $^{57}\text{Fe}_3\text{O}_4$  nanoparticles are enriched in the  $^{57}\text{Fe}$  stable isotope minimum to 66 %, which is more than 30-fold excess of the  $^{57}\text{Fe}$  content in nanoparticles of magnetite of natural isotope composition.

Figure 1a shows a spectrum of the synthesized  $^{57}\text{FeCl}_3 \cdot 6\text{H}_2\text{O}$  compound measured at  $T = 300$  K and having the form of an anomalous quadrupole doublet whose asymmetry subsides with the temperature decrease. Such form and behavior of a spectrum are typical for the  $\text{FeCl}_3 \cdot 6\text{H}_2\text{O}$  compound [6] and are due to the joint manifestation of the spin-spin relaxation and the Karyagin-Goldanskii effect in this compound. No partial contributions from other iron chemical compounds were found in the spectrum. Figure 1b shows a spectrum of the  $\text{FeCl}_2 \cdot 4\text{H}_2\text{O}$  compound used in the synthesis process containing iron of the natural isotope composition (as measured at  $T = 300$  K). It has the form of a quadrupole doublet with hyperfine interaction parameters coinciding with those cited in literature for this compound [7]. Thus, similarly to the  $^{57}\text{FeCl}_3$  hydrate and  $\text{FeCl}_2$  hydrate, no additional iron-containing compounds were found.

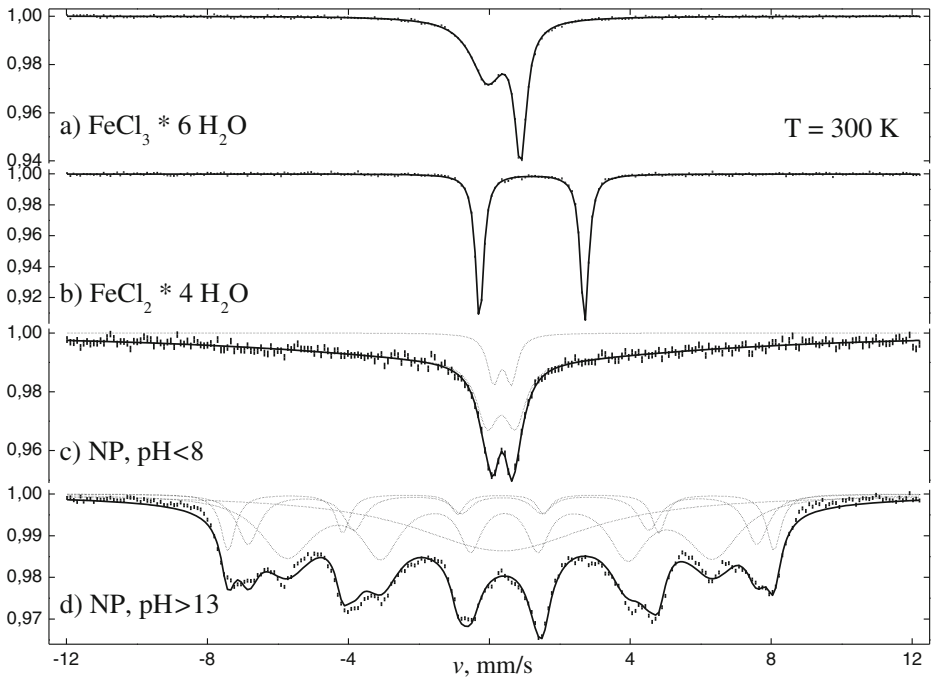


**Fig. 1** Mössbauer spectra of  $^{57}\text{Fe}$  nuclei in initial chemical agents  $^{57}\text{FeCl}_3 \cdot 6\text{H}_2\text{O}$  (a),  $^{57}\text{FeCl}_2 \cdot 4\text{H}_2\text{O}$  (b),  $^{57}\text{Fe}_3\text{O}_4$  nanoparticles synthesized via co-precipitation of these agents at pH < 8 (c), pH > 13 (d)

The performance of magnetic nanoparticles synthesized with the sol-gel method depends crucially on the PH of the solution where hydrates of iron salts are co-precipitated. To illustrate this circumstance, Fig. 1c shows a Mössbauer spectrum of  $\text{Fe}_3\text{O}_4$  nanoparticles synthesized at pH < 8, and Fig. 1d shows a Mössbauer spectrum of  $\text{Fe}_3\text{O}_4$  nanoparticles synthesized at pH > 13 at the same temperature. In both cases, the same chemical agents were co-precipitated in the same ratio ( $\text{Fe}^{2+}:\text{Fe}^{3+} = 1:2$ ). The characteristic shape of these spectra imply that while fine  $\text{Fe}_3\text{O}_4$  superparamagnetic particles sized less than 10 nm with the  $\text{FeOOH}$  [8] impurity were formed in the former case, in the latter case, larger ferrimagnetic  $\text{Fe}_3\text{O}_4$  nanoparticles with  $\epsilon\text{-Fe}_2\text{O}_3$  impurity [9] were produced.

In order to prepare a ferrofluid which would be suitable for injections and feature a biodegradation ability in a live organism, we have chosen  $^{57}\text{Fe}_3\text{O}_4$  magnetic nanoparticles synthesized via co-precipitation at pH = 10 which give a Mössbauer spectrum shown in Fig. 2. It coincides qualitatively with the spectra of nanoparticles from ferrofluid “fluidMAG-ARA-250” (Chemicell GmbH, Germany) we studied earlier in vivo [10] that demonstrated high biodegradation properties.

### 3 A study of physical parameters of the synthesized $^{57}\text{Fe}_3\text{O}_4$ nanoparticles

Mössbauer spectroscopy is one of the most informative methods for investigation of structural, magnetic and thermodynamic properties of magnetic nanoparticles owing to a qualitative difference in the profiles of absorption spectra, which reflect the distinctions of

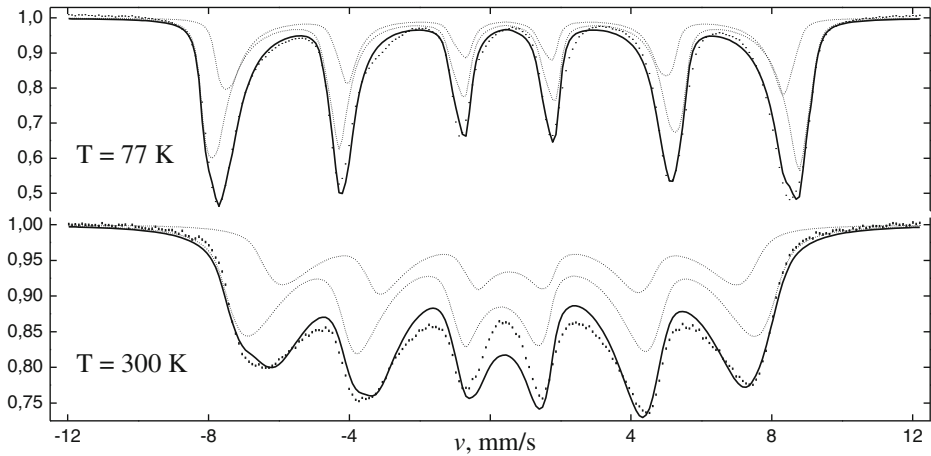


**Fig. 2** Mössbauer spectra of  $^{57}\text{Fe}$  nuclei (vertical hatches) in synthesized at pH = 10  $^{57}\text{Fe}_3\text{O}_4$  nanoparticles at liquid nitrogen temperature and room temperature, corrected with regard to the absorber thickness. Solid lines: spectra of an ensemble of chaotically oriented one-domain particles, calculated with multilevel relaxation models [14, 17]. Dashed lines: the partial contributions from ferrimagnetic sublattices A and B

the magnetic dynamics of these materials [11]. Most widely used is a method of measuring the Mössbauer spectra of magnetic nanoparticles as a function of temperature since the basic features of evolution of the spectra magnetic hyperfine structure depending on temperature are well-known as a consequence of a straight-forward double-level model of single-domain particle relaxation with axial magnetic anisotropy [12] based on the classical Neel formula for the probability of transition from one local energy minimum into another [13] in unit time:

$$p = p_0 \exp(-KV/kT), \quad (1)$$

where  $p_0$  is a constant,  $V$  is the particle volume,  $T$  is temperature,  $k$  is the Boltzmann constant. At fairly low temperatures when the nanoparticle magnetic moments are “frozen” in a local energy minima of magnetic anisotropy, the spectra show a well allowed hyperfine structure (magnetic sextet of lines for  $^{57}\text{Fe}$  nuclei, corresponding to the Zeeman splitting of nucleus energy levels in the hyperfine magnetic field  $\mathbf{H}_{hf}$ ). As temperature rises, the transitions between local states start to play an important role and when the rate of these transitions becomes comparable with the nucleus lifetime in the excited state, the magnitude and direction of  $\mathbf{H}_{hf}$  follow time variations of a particle magnetic moment and vary in time randomly, which leads to smearing of the magnetic hyperfine structure of the spectra. The most adequate model for characterization of such Mössbauer spectra transformation is a multilevel relaxation model [14] based on a quantum-mechanical specification of a uniformly magnetized particle with full spin  $S$  and energy

$$E = -KV \cos^2 \theta = -KV S_z^2 / S^2. \quad (2)$$

Here,  $K$  is an axial magnetic anisotropy constant,  $\theta$  is an angle between the direction of the uniform magnetization  $\mathbf{M}$  and the easiest magnetization axis of a particle. Then the transitions between  $(2S+1)$  stochastic states of projection  $S_z$  are caused by transverse components of a random field [14, 15].

Unfortunately, this theory provides a good description of the spectra of ferromagnetic particles only. The theory of magnetism of the ferrimagnetic nanoparticles is at the development stage nowadays. In ferrimagnets, identical atoms occupying different crystallographic positions form two interleaved magnetic sublattices with their own magnetic moments and the particle energy depends on the orientation of both moments relative to the easy axis. However, on deviation of the sublattice moments from a mutually antithetical direction, the system energy increases sharply, that is, the energy profile of the ferrimagnetic particle appears to be nearly one-dimensional and can be well described by Eq. 2. It offers a possibility to regard a spectrum of the ferrimagnetic particles in the first approximation as a sum of ferromagnetic contributions from each of the sublattices with their own hyperfine parameters and a common diffusion constant characterizing the joint relaxation process intensity. In this approximation the spectrum of superparamagnetic  $\text{Fe}_3\text{O}_4$  particles contains two components with slightly smaller isomer shifts than those of the A and B sites in bulk magnetite which can be treated within the same “ferromagnetic” (1) and (2). Another difference of magnetite nanoparticles from the bulk magnetite is the phenomenon of “metamagnetism” which results in essential transformation of the Mössbauer spectra due to specific relaxation processes [16]. As a consequence, the Verwey transition in such nanoparticles with a diameter of about or less than 10 nm may not reveal itself in the Mössbauer spectra.

Mössbauer absorption spectra of  $^{57}\text{Fe}$  nuclei in a sample of synthesized  $^{57}\text{Fe}_3\text{O}_4$  nanoparticles at room temperature and liquid nitrogen temperature are given in Fig. 2. The profile of these spectra reflects qualitatively the standard behavior of an ensemble of single-domain particles with magnetic anisotropy. At low temperature, a well allowed hyperfine magnetic structure (a magnetic sextet for  $^{57}\text{Fe}$  nuclei) is observable in the spectrum. With temperature rise the relaxation process leads to smearing of the spectra magnetic hyperfine structure. The detailed analysis of these spectra was performed with the use of a stochastic model for characterization of relaxation effects in a system of uniformly magnetized one-domain particles with energy (2) [14] extended for the presence of a quadrupolar hyperfine interaction [17].

We carried out the simultaneous mean-square analysis of the two spectra, each as a composition of two contributions of the sublattices with standard Mössbauer parameters of isomer shift – the centre of gravity of the spectrum –  $\delta$ , quadrupolar shift  $q$  and hyperfine field  $H_{hf}$ , as well as common for both sublattices diffusion/relaxation constant  $D$ , energy barrier in the anisotropy field  $KV$  and relative width of Gaussian distribution of numbers of nanoparticles over their diameters  $\sigma/d$ . Found values of effective absorber thickness  $\sigma$  at two temperatures allows us to estimate the Debye temperature  $T_D$  for nanoparticles and so the concentration of the resonant isotope in their substance  $n_{57\text{Fe}}$ . Solid lines in Fig. 2 show the result of the analysis, and Tables 1 and 2 gives the corresponding values of the parameters.

#### 4 A study of biocompatibility and biodegradability of synthesized $^{57}\text{Fe}_3\text{O}_4$ nanoparticles

Recently, a potentiality of Mössbauer spectroscopy for studying the biodegradation process of magnetic nanoparticles in vivo in mouse liver was demonstrated [18]. Magnetic nanoparticles in the form of ferrofluid were administrated intravenously to a mouse. The Mössbauer study of the mouse liver samples has shown that in addition to the sextet of lines related to the injected nanoparticles there appears an intense doublet of lines in the spectra shortly after the particles were administered. Further analysis revealed that the doublet

**Table 1** Mössbauer parameters, corresponding to the spectra of the initial chemical agents and synthesized nanoparticles, shown in Fig. 1: isomer shift  $\delta$ , quadrupolar shift  $q$  and hyperfine field  $H_{hf}$  as well as relative contribution  $\sigma$  of the partial sub-spectra to the result spectra. In brackets, mean-root-square errors of the parameters in the last sign are given

|                                   | $\delta$ , mm/s | $q$ , mm/s | $H_{hf}$ , kOe | $\sigma$ , % |
|-----------------------------------|-----------------|------------|----------------|--------------|
| $\text{FeCl}_3$                   | 0.416 (4)       | 0.491 (4)  | 0              | 100          |
| $\text{FeCl}_2$                   | 1.215 (1)       | 1.490 (1)  | 0              | 100          |
| $\text{Fe}_3\text{O}_4$ (pH < 8)  | 0.2 (2)         | -0.2 (2)   | 160 (20)       | 93 (2)       |
|                                   | 0.37 (2)        | 0.25 (2)   | 0              | 7 (2)        |
| $\text{Fe}_3\text{O}_4$ (pH > 13) | 0.33 (1)        | 0.00 (1)   | 481 (1)        | 10 (1)       |
|                                   | 0.36 (1)        | -0.06 (1)  | 376 (1)        | 42 (1)       |
|                                   | 0.36 (1)        | 0.02 (1)   | 449 (1)        | 14 (1)       |
|                                   | 0.36 (2)        | 0.00 (2)   | 0              | 32 (1)       |

consists of two components related to the formation of iron-containing proteins and superparamagnetic behavior of the injected nanoparticles. Using a combined analysis of three Mössbauer spectra measured at different external conditions for each sample, these components were separated and the evolution with time of each component was characterized [10]. Hence, the proposed method makes it possible, by the evolution of the shape of the relaxation Mössbauer spectra of the investigated body, to control both a process of reducing the concentration of exogenous superparamagnetic nanoparticles and a simultaneous increase in the concentration of endogenous iron-containing proteins. In [5] we tried to assess experimentally the feasibility of the method for solving more challenging problems - control of biodegradation of magnetic nanoparticles in the brain.  $\text{Fe}_3\text{O}_4$  based ferrofluid was injected transcranially in the ventricle of the rat brain. Three months after the injection the rat was sacrificed and the brain was studied with the Mössbauer spectroscopy and histological Perls Prussian blue method. A joint analysis of histological and Mössbauer data confirms that  $\text{Fe}_3\text{O}_4$  superparamagnetic nanoparticles, which constituted about 91 % of the iron of the ferrofluid, were removed from the brain while the concomitant chemical compound, containing ferric ion in the high-spin state, remained intact. In this paper, we repeated this experiment with our new 66 %  $^{57}\text{Fe}$ -enriched  $\text{Fe}_3\text{O}_4$  nanoparticles. The procedure for the transcranial injection of nanoparticles into the brain of rats and preparation of samples for the Mössbauer study is fully consistent with the procedure described in [5]. The Mössbauer spectra of the initial  $^{57}\text{Fe}_3\text{O}_4$  based ferrofluid and the rat brain measured in two hours and one week after the transcranial injection of the magnetic ferrofluid are shown in Fig. 3, and corresponding values of the parameters are presented in Table 3. As can be seen, as early as 2 h after the injection of  $^{57}\text{Fe}_3\text{O}_4$  nanoparticles into the brain, a paramagnetic component starts to be formed in the centre of the spectrum in addition to the Zeeman sextet corresponding to initial nanoparticles, and in a week after the injection, there is only this paramagnetic component left and the sextet practically disappears. We are studying the nature of this paramagnetic component now; however, we may already assert that the synthesized magnetic  $^{57}\text{Fe}_3\text{O}_4$  nanoparticles undergo intensive biodegradation in live brain and, therefore, can be regarded as a promising target for radionuclide-free Mössbauer brachytherapy.

**Table 2** Mössbauer parameters, corresponding to the spectra of nanoparticles at liquid nitrogen and room temperatures, shown in Fig. 2: isomer shift  $\delta_{A,B}$ , quadrupolar shift  $q_{A,B}$  and hyperfine field  $H_{hfA,B}$  for the ferrimagnetic sublattices A and B as well as diffusion constant  $D$ , energy barrier in the anisotropy field  $KV_{\bar{d}}$  for the central value  $\bar{d}$  of Gaussian distribution of numbers of nanoparticles over their diameters and its relative width  $\sigma d/\bar{d}$ ; values of the effective absorber thickness  $\sigma$  for nanoparticles, their Debye temperature  $T_D$  and the concentration of the resonant isotope in their substance  $n_{57\text{Fe}}$  are also presented

|                                              | T = 78 K   | T = 300 K |
|----------------------------------------------|------------|-----------|
| $KV_{\bar{d}}$ , K                           | 418 (3)    | 418 (3)   |
| $\sigma d/\bar{d}$                           | 0.276 (2)  | 0.276 (2) |
| $q_A$ , mm/s                                 | 0.352 (1)  | 0.352 (1) |
| $q_B$ , mm/s                                 | 0.356 (1)  | 0.356 (1) |
| $D$ , mm/s                                   | 0          | 0.817 (6) |
| $H_{hfA}$ , kOe                              | 524.57 (3) | 513.3 (3) |
| $H_{hfB}$ , kOe                              | 498.14 (7) | 461.1 (5) |
| $\delta_A$ , mm/s                            | 0.4593 (3) | 0.318 (2) |
| $\delta_B$ , mm/s                            | 0.4419 (5) | 0.554 (4) |
| $\sigma$                                     | 25.89 (1)  | 24.71 (3) |
| $T_D$ , K                                    | 660 (10)   | 660 (10)  |
| $n_{57\text{Fe}}$ , $10^{21} \text{cm}^{-3}$ | 9 (1)      | 9 (1)     |

**Table 3** Mössbauer parameters, corresponding to the spectra of the initial  $^{57}\text{Fe}_3\text{O}_4$ -based ferrofluid and the rat brain in two hours and one week after the transcranial injection of the ferrofluid, shown in Fig. 3: for the magnetic contribution of nanoparticles parameters are named in the caption of Table 2; for paramagnetic phase they are isomer shift  $\delta^{(p)}$ , quadrupolar shift  $q^{(p)}$  and Lorentz line width  $\Gamma^{(p)}$  as well as the effective absorber thickness  $\sigma^{(p)}$  and the concentration of the resonant isotope  $n_{57\text{Fe}}^{(p)}$ . Dashes are placed instead of uncertain values

|                                                    | NP        | 2 hours   | 1 week    |
|----------------------------------------------------|-----------|-----------|-----------|
| $KV_{\bar{d}}$ , K                                 | 418 (3)   | 230 (20)  | 200 (100) |
| $\sigma d/\bar{d}$                                 | 0.276 (2) | –         | –         |
| $q_A$ , mm/s                                       | 0.352 (1) | 0.4 (1)   | 0.5 (4)   |
| $q_B$ , mm/s                                       | 0.356 (1) | 0.4 (1)   | 0.5 (8)   |
| $D$ , mm/s                                         | 0.817 (6) | 0.11 (2)  | –         |
| $H_{hfA}$ , kOe                                    | 513.3 (3) | 510 (5)   | 510 (20)  |
| $H_{hfB}$ , kOe                                    | 461.1 (5) | 460 (10)  | 460 (40)  |
| $\delta_A$ , mm/s                                  | 0.318 (2) | 0.32 (2)  | 0.3 (2)   |
| $\delta_B$ , mm/s                                  | 0.554 (4) | 0.55 (5)  | 0.6 (4)   |
| $\sigma$                                           | 24.71 (3) | 0.512 (4) | 0.030 (2) |
| $n_{57\text{Fe}}$ , $10^{16} \text{cm}^{-3}$       | 9e5 (1e5) | 216 (2)   | 15 (1)    |
| $q^{(p)}$ , mm/s                                   | –         | 0.19 (2)  | 0.33 (2)  |
| $\delta^{(p)}$ , mm/s                              | –         | 0.38 (2)  | 0.37 (1)  |
| $\Gamma^{(p)}$ , mm/s                              | –         | 0.42 (8)  | 0.47 (5)  |
| $\sigma^{(p)}$                                     | –         | 0.018 (1) | 0.015 (1) |
| $n_{57\text{Fe}}^{(p)}$ , $10^{16} \text{cm}^{-3}$ | –         | 21 (2)    | 21 (2)    |



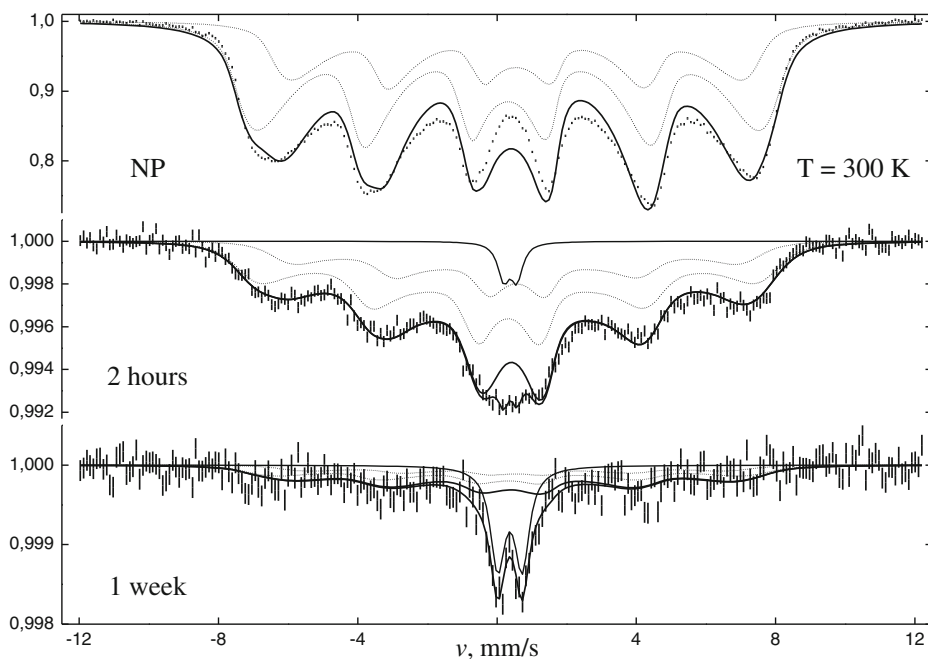


**Fig. 3** Mössbauer spectra of the initial  $^{57}\text{Fe}_3\text{O}_4$ -based ferrofluid and the rat brain measured in 2 hours and 1 week after the transcranial injection of the magnetic ferrofluid

**Acknowledgments** The work was partly supported by the Russian Foundation for Basic Research and the Ministry of Education and Science of Russia.

## References

1. Liu, Y., Sozontov, E., Safronov, V., Gutman, G., Strumban, E., Jiang, Q., Li, S.: 3D polymer gel dosimetry and Geant4 Monte Carlo characterization of novel needle based X ray source. *J. Phys.: Conf. Ser.* **250**, 012069 (2010)
2. Le Duc, G., Miladi, I., Alric, C., Mowat, P., Brauer Krisch, E., Bouchet, A., Khalil, E., Billotey, C., Janier, M., Lux, F., Epicier, T., Perriat, P., Roux, S., Tillement, O.: Toward an image-guided microbeam radiation therapy using gadolinium-based nanoparticles. *ACS Nano.* **5**(12), 9566–9574 (2011). doi:[10.1021/nm202797h](https://doi.org/10.1021/nm202797h)
3. Mills, R.L., Walter, C.W., Venkataraman, L., Pang, K., Farrell, J.J.: A novel cancer therapy using a Mössbauer-isotope compound. *Nature* **336**, 787–789 (1988)
4. Brenner, D.J., Geard, C.R., Hall, E.J.: Mössbauer cancer therapy doubts. *Nature* **339**, 185–186 (1989)
5. Polikarpov, D.M., Cherepanov, V.M., Gabbasov, R.R., Chuev, M.A., Mischenko, I.N., Korshunov, V.A., Panchenko, V.Y.: Efficiency analysis of clearance of two types of exogenous iron from the rat brain by Mössbauer spectroscopy. *Hyperfine Interact.* **218**(1–3), 83–88 (2013)
6. Thrane, N., Trumpy, G.: Spin-spin relaxation and Karyagin-Goldanskii effect in  $\text{FeCl}_3 \cdot 6\text{H}_2\text{O}$ . *Phys. Rev. B* **1**(11), 153–155 (1970)
7. Hazony, Y., Hang Nam, Ok.: 3d density distribution and crystal field in  $\text{FeCl}_2$ : A Mössbauer study. *Phys. Rev.* **188**(2), 591–593 (1969)
8. Ganguly, B., Muggins, F., Feng, Z., Huffman, G.: Anomalous recoilless fraction of 30-Å-diameter  $\text{FeOOH}$  particles. *Phys. Rev. B* **49**(5), 3036–3042 (1994)

9. Machala, L., Tucek, J., Zboril, R.: Polymorphous transformations of nanometric iron(III) oxide: A review. *Chem. Mater.* **23**, 3255–3272 (2011)
10. Gabbasov, R.R., Cherepanov, V.M., Chuev, M.A., Polikarpov, M.A., Nikitin, M.P., Deyev, S.M., Panchenko, V.Y.: Biodegradation of magnetic nanoparticles in mouse liver from combined analysis of Mössbauer and magnetization data. *IEEE Trans. Magn.* **49**(1), 394–397 (2013)
11. Chuev, M.A., Hesse, J.: Non-equilibrium magnetism of single-domain particles for characterization of magnetic nanomaterials. In: Tamayo, K.B. (ed.) *Magnetic Properties of Solids*, pp. 1–104. Nova Science Publishers, New York (2009)
12. Wickman, H.H.: Mössbauer effect methodology. In: Gruverman, I.J. (ed.) v.2, Plenum Press, New York (1966)
13. Néel, L.: Theory of the magnetic after-effect in ferromagnetics in the form of small particles, with applications to baked clays. *Ann. Géophys.* **5**, 99 (1949)
14. Jones, D.H., Srivastava, K.K.P.: Many-state relaxation model for the Mössbauer spectra of superparamagnets. *Phys. Rev.* **B34**, 7542–7548 (1986)
15. Chuev, M.A.: Mössbauer spectra of magnetic nanoparticles in the model of continuous diffusion and precession of uniform magnetization. *JETP Lett.* **83**(12), 572–577 (2006)
16. Chuev, M.A.: On the shape of gamma\_resonance spectra of ferrimagnetic nanoparticles under conditions of metamagnetism. *JETP Lett.* **98**(8), 465–470 (2013)
17. Chuev, M.A.: Multi-level relaxation model for describing the Mössbauer spectra of single-domain particles in the presence of quadrupolar hyperfine interaction. *J. Phys. Condens. Matter.* **23**, 426003 (2011)
18. Nikitin, M., Gabbasov, R., Cherepanov, V., Chuev, M., Polikarpov, M., Panchenko, V., Deyev, S.: Magnetic nanoparticle degradation in vivo studied by Mössbauer spectroscopy. *Am. Inst. Phys. Conf. Proc. Ser.* **1311**, 401–407 (2010)